HeII to Hα correlation for WR-rich regions, luminous HII regions, and even some AGN's

Grigorii Smirnov-Pinchukov

April 5, 2017

1 Introduction

I came to AIP, Potsdam, on March 7th 2017. My task was to check HeII4685/Hα correlation in WR-rich regions and luminous HII regions.

WR-rich regions were found previously by Miralles-Caballero et al., 2016. List of HII regions in CALIFA data was prepared by S.F. Sanchez. I selected 250 most luminous HII regions with $EW_{H\alpha} < -30$Å from galaxies, presented in CALIFA DR3 COMB cubes. Their redshifts for initial fit guess were taken from the table prepared by C.J. Walcher. The distances were estimated using infall-corrected redshifts by S. Bekeraite as $D = zc/H$, assuming $H = 70\ kms^{-1}/Mpc,\ c = 3 \cdot 10^5\ kms^{-1}$. I analyzed only 32 WR-rich regions with COMB cubes and infall-corrected redshifts available.

In the last 2 days of the internship I added 78 HII regions from the list with $EW_{H\alpha} < -10$ and $Flux_{H\alpha} \geq 3 \cdot 10^{-14} erg/s$ to cover Hαluminosities less than $10^{41} ergs/s$.

The analysis was made using self-written IDL scripts, PyParadise software (J. Walcher et al.) and IRAF splot routine. To make PyParadise fit better I prepared a Python script PARADISE_AUTOFLUX.PY, that makes guesses for fluxes, searching for emission lines in residuals.

2 Results

For each region I prepared:

1. Spectrum created by adding 16 1×1 arcsec spaxels of a square aperture around each selected region, its raster plot, and localization (*GIF* folder).

2. Separate parameter files with redshift-corrected velocity guesses.

3. Each spectrum was fitted using PyParadise application with a standard PyParadise output (*Paradise* folder).

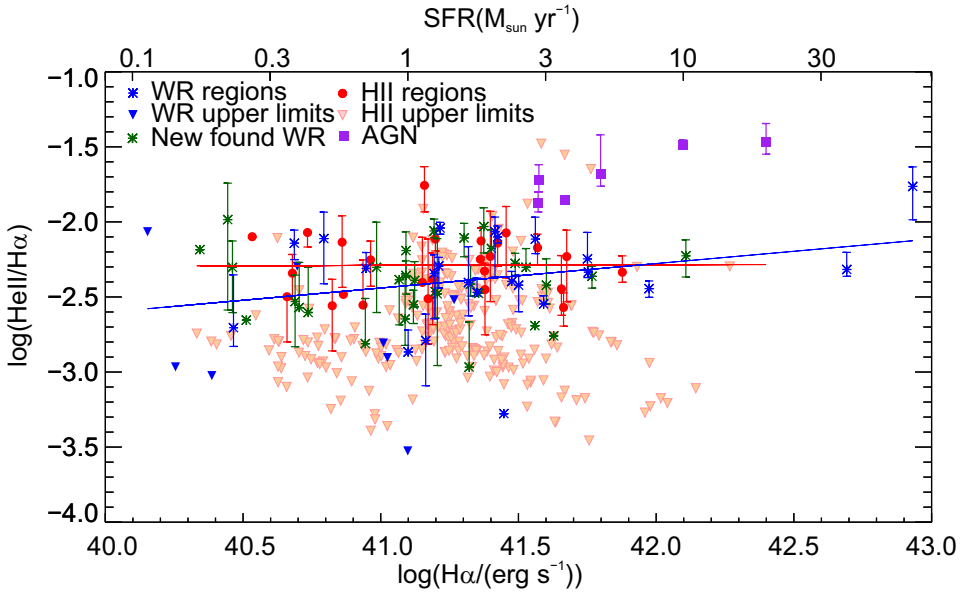

Figure 1: HeII4685 to Hα plot for different regions.

4. Each region was checked for HeII emission and WR blue bump by eye. All regions with HeII were fitted using IRAF splot routine.

The PyParadise output was analyzed by self-written IDL scripts. I present HeII/Hα – Hα plot (fig. 1) as well as a lot of other line-to-Hα plots (fig. 4), BPT-diagram (fig. 2) and SII ratio plot (fig. 3).

3 Discussion

HeII fluxes were found for 23 (of 32) WR-rich regions and 62 (of 328) luminous HII regions. For all other regions, I present upper limits.

6 luminous HII regions with significant HeII and without significant WR bumps appear to be AGN's. They lay higher that all other regions on HeII/Hα diagram with logHeII/Hα around -1.7.

Most of the WR-rich regions have logHeII/Hα around -2.4, but some regions don't have significant HeII.

I found a group of HII regions that hadn't been previously noticed as WR-rich regions. They appear to show the same properties as previously found WR-rich regions. Anyway, there is still a number of luminous HII regions with a significant HeII emission without significant AGN or WR features. Most of luminous HII regions (266/328) don't show HeII emission.

The Ha luminosities were then converted to total SFRs, using the updated calibration of Tamblyn, & Kennicutt, Congdon (1994) assuming $SFR = L(H\alpha\ erg\ s^{-1})/(1.26 \cdot 10^{41}) \Rightarrow \log SFR = \log L(H\alpha\ erg\ s^{-1}) - 41.1$

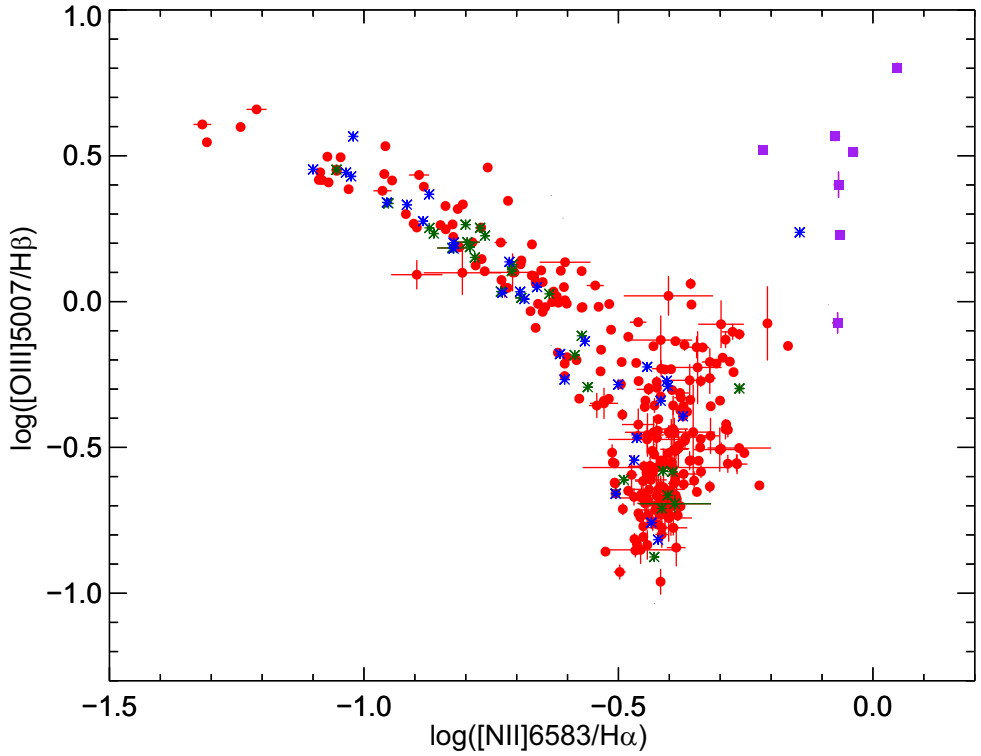

Figure 2: BPT-diagram. Blue and green asterisks – WR regions – tend to the low-metallicity band.

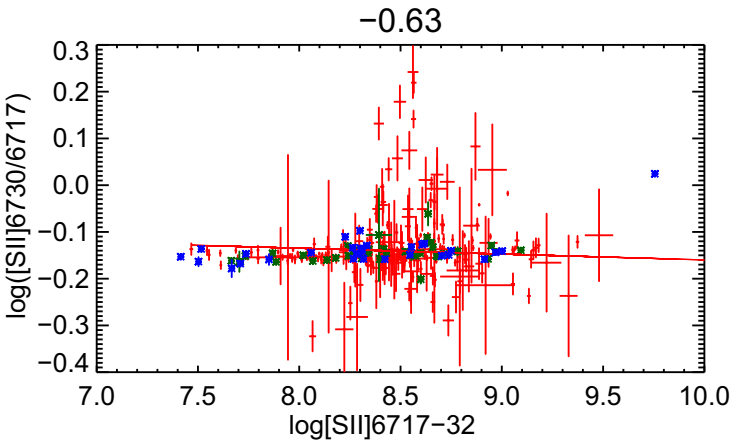

Figure 3: [SII]6730/6717

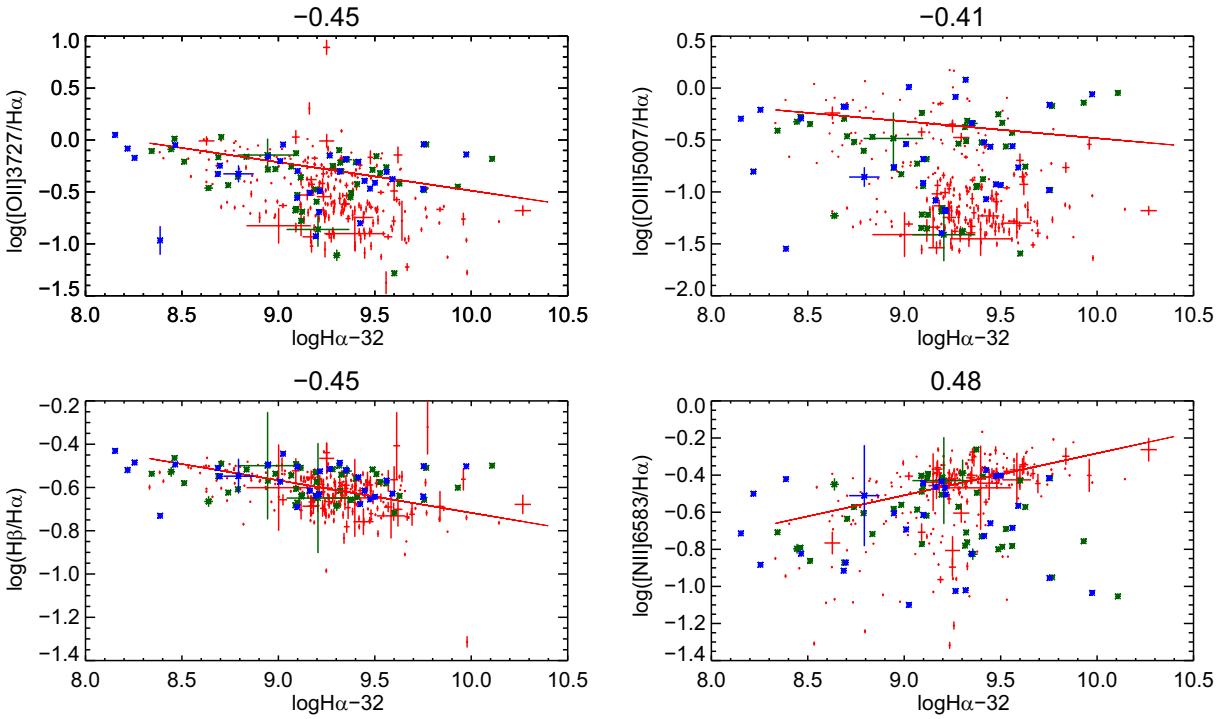

Figure 4: [OII]3727, [OIII]5007, Hβ and [NII]6583 to Hα correlations.

On the BPT diagram (fig. 2) WR-rich regions group in the low-metallicity photoionization band. Are there different ionization properties or really low-metallicity regions?

On the SII diagram (fig. 3) WR-rich region group around $\log([\mathrm{SII}]6730/6717) \simeq -0.15$ with significantly lower dispersion than HII regions.

4 What more could be done

1. Physical modeling of WR-rich HII regions.
2. Detailed study of abundances and physical properties.
3. What does cause HeII emission of red regions on fig. 1?